

5.8 Auger Electron Spectroscopy (AES)

5.8.1 The Auger Process

X-ray and high energy electron bombardment of atom can create core hole

Core hole will eventually decay via either

(i) photon emission (x-ray fluorescence -XRF)

more likely for deep core hole (high BE)

high Z elements

or (ii) radiationless internal rearrangement (Auger process)

more likely for shallow core hole (low BE)

low Z elements (almost exclusively for $Z < 15$)

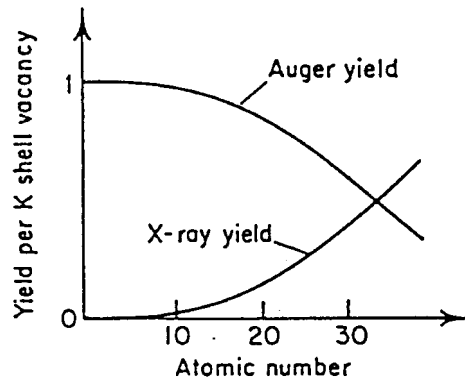
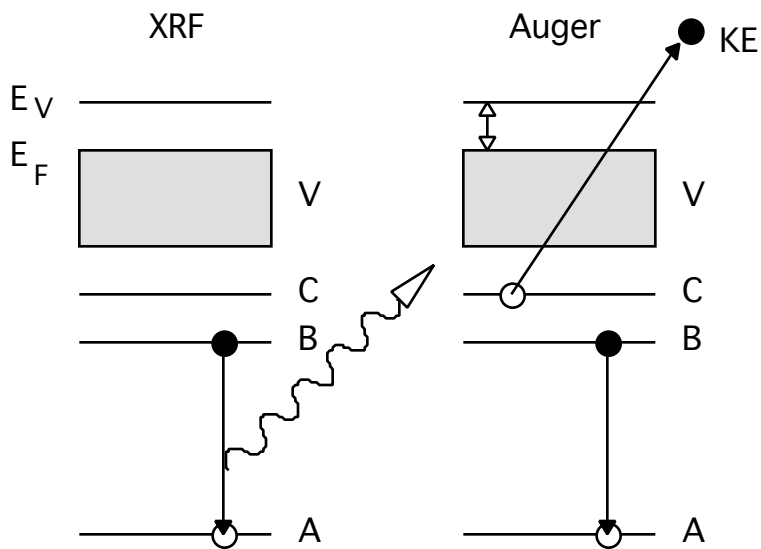


Fig. 44. The relative probabilities of X-ray emission and Auger electron emission in the decay of K (1s) holes in the lighter elements.

Auger process is a *three electron process* and leaves atom *doubly-ionized*

- occurs independently of incident excitation (doesn't "compete" with photoemission)



- Photon not much use for surface analysis since propagates large distances in solid (but is used for x-ray microprobe analysis in SEM/TEM)
- Auger electrons produced with similar kinetic energies to photoelectrons so similar surface sensitivity
- Initial core hole can be generated by *x-rays*

see Auger peaks in XPS

or *electrons* (most common in AES)

spectrum contains Auger, incident and inelastically scattered electrons

but *no photoemission* peaks!

In simple, one-electron picture (ignoring *relaxation* or *final state* effects),

X – ray photon	h	$E_A - E_B$	
Auger electron	KE	$\underbrace{E_A - E_B}_{\text{energy gained by core-hole annihilation}}$	$-\underbrace{E_C}_{\text{energy needed to overcome BE of Auger electron}} -$

Table 4.2. Binding energies of some elements

Z	El	1s _{1/2} K	2s _{1/2} L ₁	2p _{1/2} L ₂	2p _{3/2} L ₃	3s _{1/2} M ₁	3p _{1/2} M ₂	3p _{3/2} M ₃	3d _{3/2} M ₄	3d _{5/2} M ₅
1	H	14								
2	He	25								
3	Li	55								
4	Be	111								
5	B	188			5					
6	C	284			6					
7	N	399			9					
8	O	532	24		7					
9	F	686	31		9					
10	Ne	867	45		18					
11	Na	1072	63		31	1				
12	Mg	1305	89		52	2				
13	Al	1560	118	74	73	1				
14	Si	1839	149	100	99	8				
15	P	2149	189	136	135	16	10			
16	S	2472	229	165	164	16	8			
17	Cl	2823	270	202	200	18	7			
18	Ar	3202	320	247	245	25	12			
19	K	3608	377	297	294	34	18			
20	Ca	4038	438	350	347	44	26		5	
21	Sc	4493	500	407	402	54	32		7	
22	Ti	4965	564	461	455	59	34		3	
23	V	5465	628	520	513	66	38		2	
24	Cr	5989	695	584	577	74	43		2	
25	Mn	6539	769	652	641	84	49		4	
26	Fe	7114	846	723	710	95	56		6	
27	Co	7709	926	794	779	101	60		3	
28	Ni	8333	1008	872	855	112	68		4	
29	Cu	8979	1096	951	932	120	74		2	
30	Zn	9659	1194	1044	1021	137	90		9	
31	Ga	10367	1299	1144	1117	160	106		20	
42	Mo	20000	2866	2625	2520	505	410	393	208	205
46	Pd	24350	36304	3330	3173	670	559	531	340	335
48	Ag	25514	3806	3523	3351	718	602	571	373	367
73	Ta*	67416	11681	11136	11544	*566	*464	*403	*24	*22
79	Au*	80724	14352	13733	14208	*763	*643	*547	*88	*84

* 4s, 4p et 4f levels indicated, respectively

In theory, can work out approximate KE of each Auger electron from tables

Example:

Z	BE (eV)		
	1s	2p _{1/2}	2p _{3/2}
8 Oxygen	532	24	7
9 Fluorine	686	31	9

Core hole ionization of 1s electron BE in O = 532 eV (E_A)

BE of 2p_{1/2} electron in O = 24 eV (E_B)

BE of $2p_{3/2}$ electron in O = 7 eV (E_C)

Auger electron KE (E_{ABC}) in O = 532 - 24 - 7 = 501 eV

Sometimes BE is "scaled" to a value between Z (O) and (Z+1) (F) to account for relaxation effects

$$KE = E_A(Z) - E_B(Z + 0.5) - E_C(Z + 0.5) - E_{ABC}$$

$$= 532 - 27.5 - 8 = 496.5 \text{ eV}$$

Observe increases in KE with Z for given set of transitions (more energy available from core-hole relaxation)

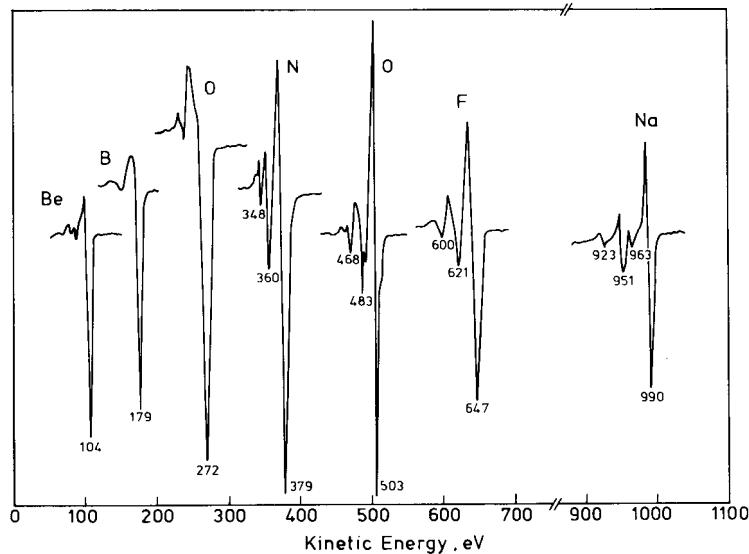


Figure 3.6 Auger spectra in the differential distribution characteristic of the lightest elements. The principal peak is the $KL_{2,3}L_{2,3}$. The relative intensities are not to scale. (Reproduced from Davis *et al.*⁹ by permission of Perkin-Elmer Corporation)

While KE of Auger electron is *independent of excitation energy*, apparent BE will change depending upon x-ray $h\nu$ in XPS (only)

Experimental KE of O KLL Auger electron is 508.3 eV (fixed)

Apparent BE of O Auger with $h\nu = 1253.6 \text{ eV}$ is 745.3 eV

Apparent BE of O Auger with $h\nu = 1486.6 \text{ eV}$ is 978.3 eV

$$= 233.0 \text{ eV} = h\nu - (Al K_{1,2} - Mg K_{1,2})$$

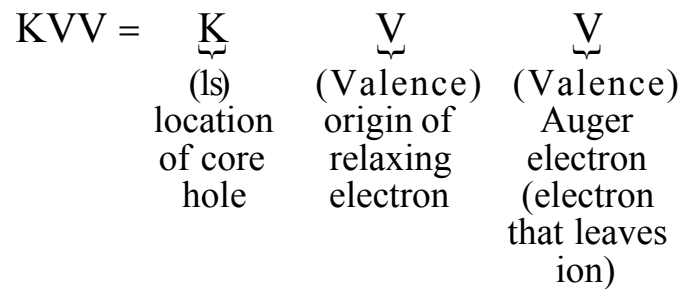
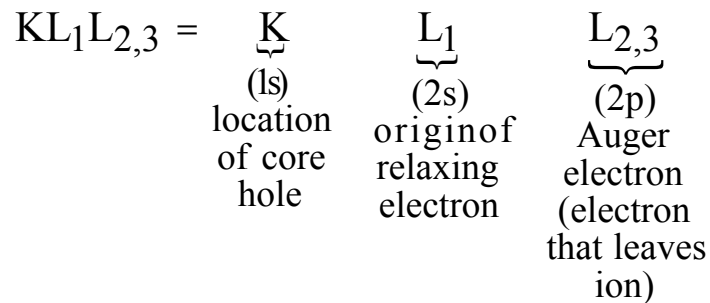
5.8.2 Auger Transition Notation

Auger electrons designated by x-ray notation as KLL, $KL_1L_{2,3}$, $L_{2,3}M_{2,3}M_{4,5}$ or KVV... etc.

First letter - initial core hole location

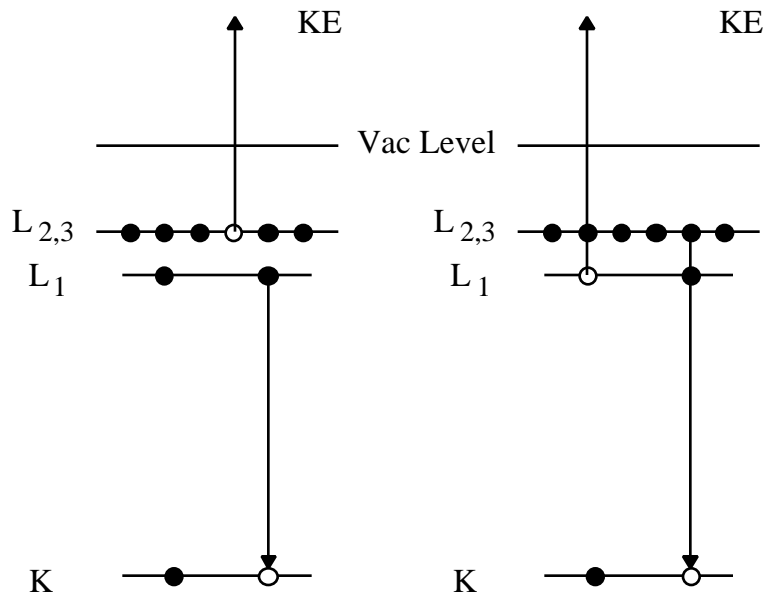
Second letter - initial location of relaxing electron

Third letter - location of second hole (initial location of Auger electron)



In reality, cannot identify exact origin of Auger electron since

$$\begin{aligned} KE &= (E_A - E_B) - E_C \\ &= E_A - (E_B + E_C) \end{aligned}$$



Usual to think of left-hand process

Regardless, Auger transition is characterized by (a) presence of core hole and (b) location of two final state holes

For just K shell hole:

For 3 levels, KL_1L_1 , $KL_1L_{2,3}$, $KL_{2,3}L_{2,3}$

For 4 levels KL_1L_1 , $KL_1L_{2,3}$, $KL_{2,3}L_{2,3}$, KL_1M_1 , $KL_{2,3}M_1$, KM_1M_1

Auger (electron or x-ray excited) spectra contain closely-spaced groups of *multiple peaks!*

5.8.3 The Probability of Auger Emission

AES usually performed using electron source not x-rays (experimentally simpler and cheaper)

Basic steps in Auger electron creation:

- (1) Creation of core hole
- (2) Creation of Auger electron by relaxation

Probability (cross-section) of creating core hole electron through (1)

$$= \text{Constant} \frac{C \frac{E_i}{E_A}}{E_A^2}$$

where E_i is incident electron beam energy, E_A is core hole BE and C is a constant (depends on core level)

typical values 10^{-3} to 10^{-4}

many incident electrons needed for 1 ionization event

reaches maximum about $3 \cdot E_A$

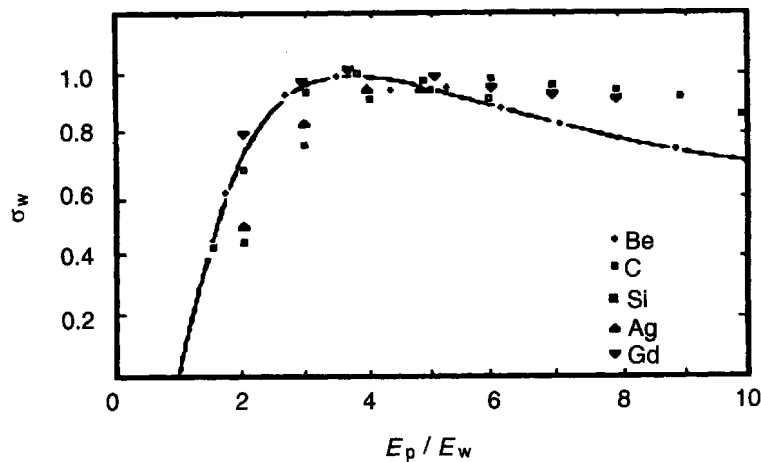


Figure 4.5. Variation of the ionization cross-section with the ratio of primary electron beam energy E_p and core level energy E_w

For maximum sensitivity of KLL Auger electron with KE 1000 eV, set incident beam energy to ~ 3000 eV

Probability of Auger emission (probability) through process (2) following core hole creation competes with XRF

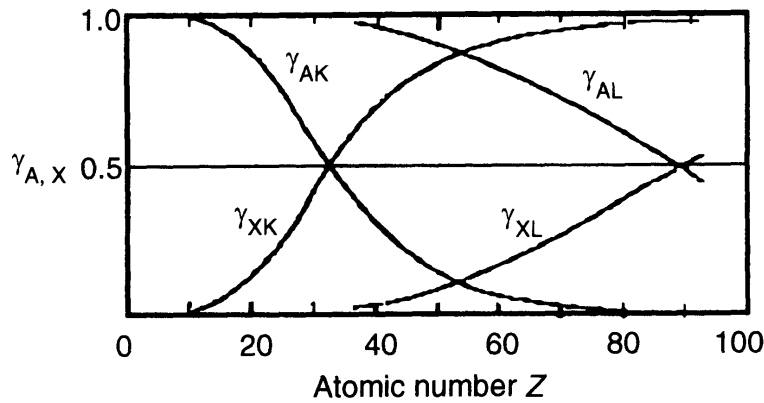


Figure 4.6. Emission probability of an Auger electron (A) or photon (X)

Auger emission favored for low Z elements

Probability varies with Z and core hole location (K, L, M...)

5.8.4 Backscattered and Secondary Electrons

Typical E_i may be 3 - 30 keV - may penetrate 100's Å into solid

Many inelastic collisions produce many *low energy secondary electrons*, additional *Auger electrons* or *photons*

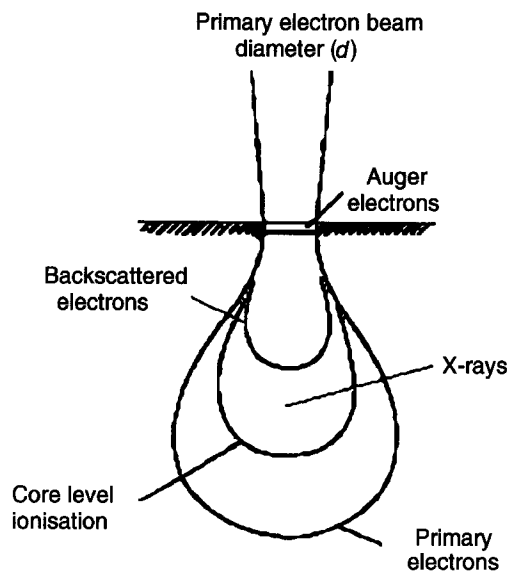


Figure 4.1. Distribution (schematic) of primary, backscattered and Auger electrons together with X-rays

Such backscattered electrons contribute to spectrum - can originate from deep within solid

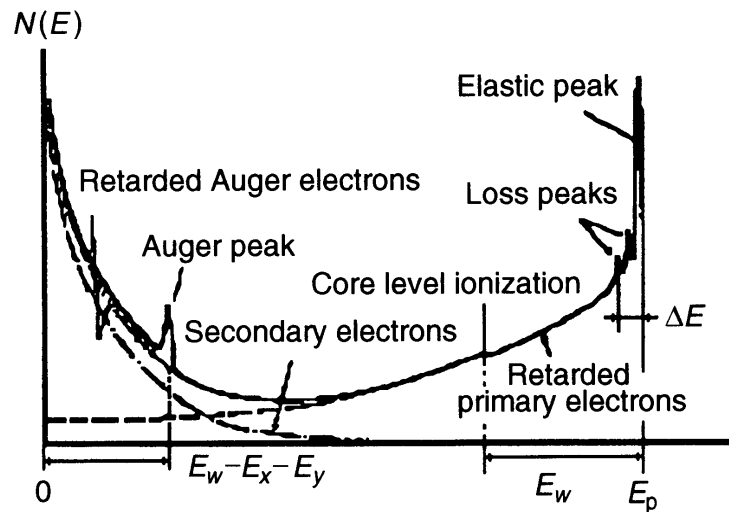
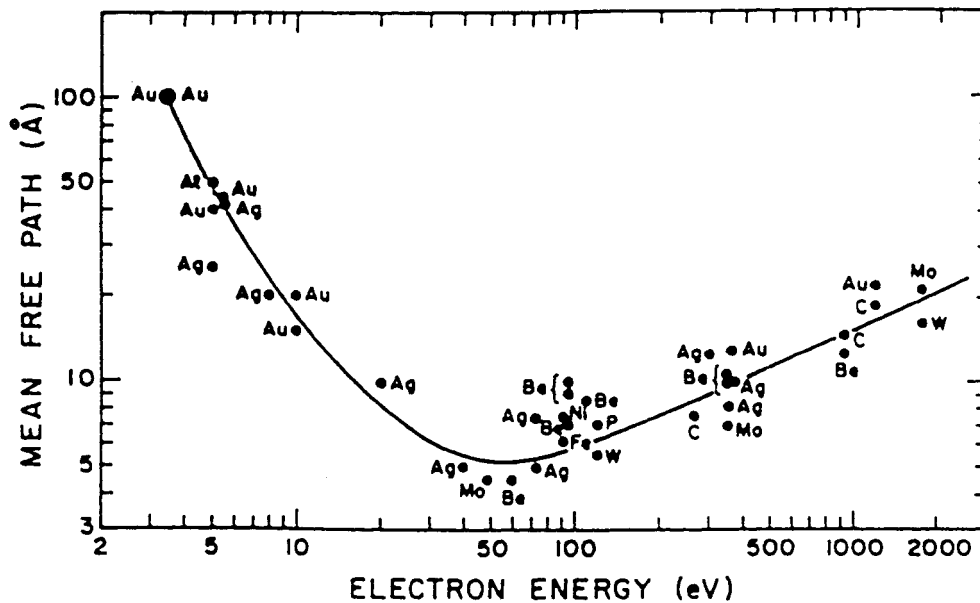


Figure 4.3. Schematic representation of an Auger spectrum

True Auger electrons behave according to "universal curve" as in XPS



$$I = I_0 \exp \frac{-d}{\cos} \qquad \ln \frac{I}{I_0} = \frac{-d}{\cos}$$

When $\ln \frac{I}{I_0} = 0.05$ (95 % electrons), $d \approx 3$

Consequence?

Auger spectrum contains many unwanted background electrons - Auger peaks appear as small features on intense inelastic background

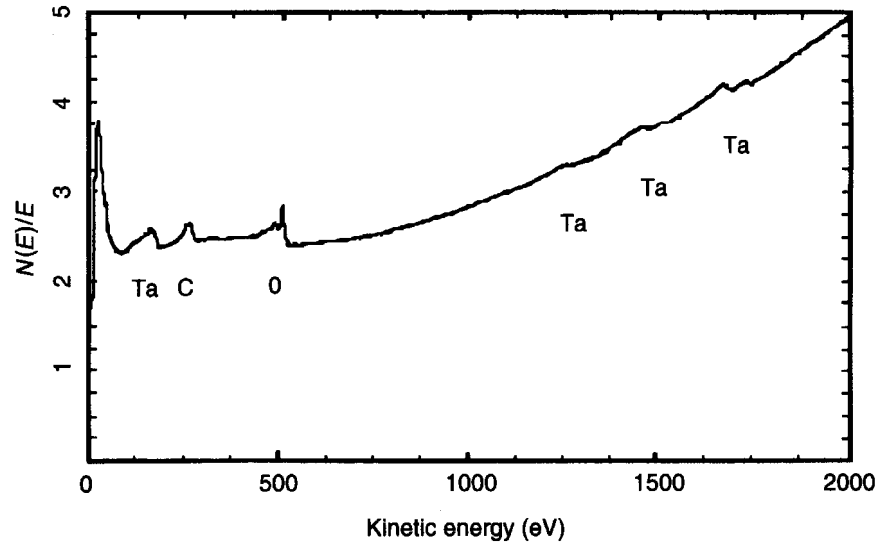


Figure 4.14. Typical survey spectrum Ta_2O_5 as a result of a point analysis

Often spectra are differentiated $N(E)$ $N'(E)$ or $dN(E)/dE$

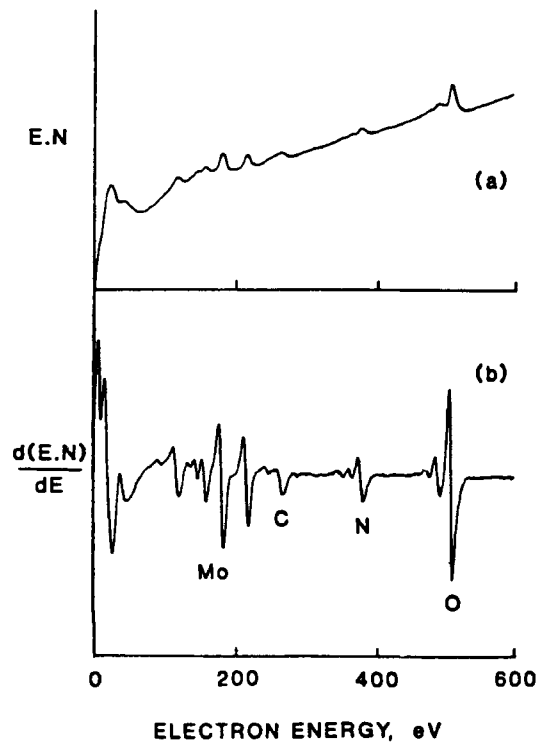


Figure 3.3 Auger spectra from a contaminated molybdenum surface in the (a) undifferentiated and (b) differentiated modes. (Reproduced from Grant³ by permission of John Wiley & Sons)

5.8.5 Chemical Shifts in AES

The equation

$$KE = E_A - E_B - E_C -$$

is a "*one-electron approximation*"

Should include *hole-hole interaction energy* (H) and *screening or polarization energy* of the surrounding atoms (S)

$$KE = E_A - E_B - E_C - H - S -$$

As in XPS, energy levels sensitive to "*chemical environment*" of atom in solid - chemical shift

But source of shift can come from perturbation of E_A , E_B , E_C , H or S?

In general, difficult to assign one chemical shift to AES spectra

Rely on "*fingerprint*" spectra

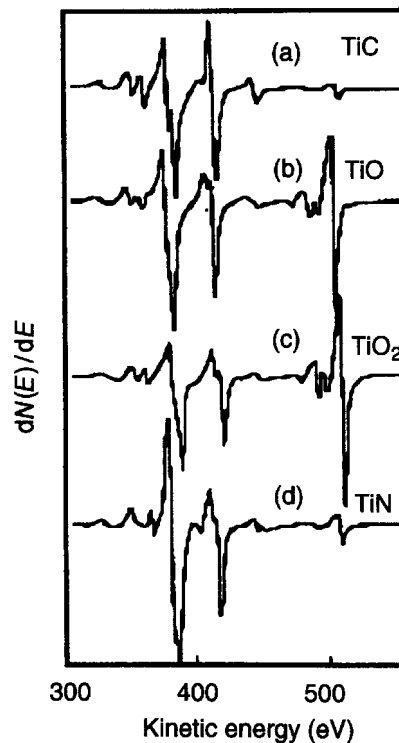


Figure 4.15. Differentiated AES spectra of Titanium as function of their kinetic energy for: (a) TiC; (b) TiO; (c) TiO₂ and (d) TiN

Can see chemical shifts in AES but

Each of the three electrons involved can be associated with multiple final states or relaxation effects

Peaks are broadened compared with photoemission peaks

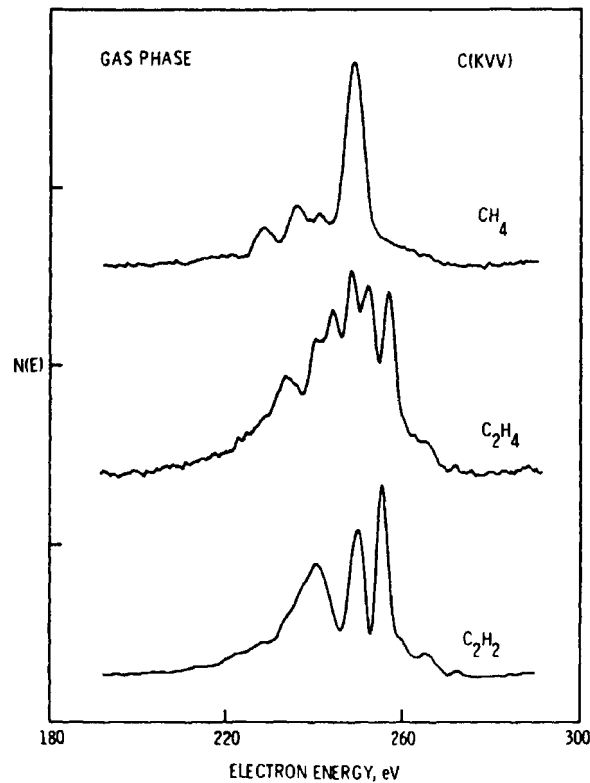


Figure 3.12 Carbon *KVV* Auger spectra in the undifferentiated mode from gaseous methane, ethylene and acetylene, showing the differences in the fine structure. (Reproduced from Houston and Rye¹³ by permission of the American Institute of Physics)

Presence of loss features (plasmons, phonons) may confuse

AES data vastly complicated by *multiple final states* and possible intensity shifts

Auger spectra difficult to assign or calculate

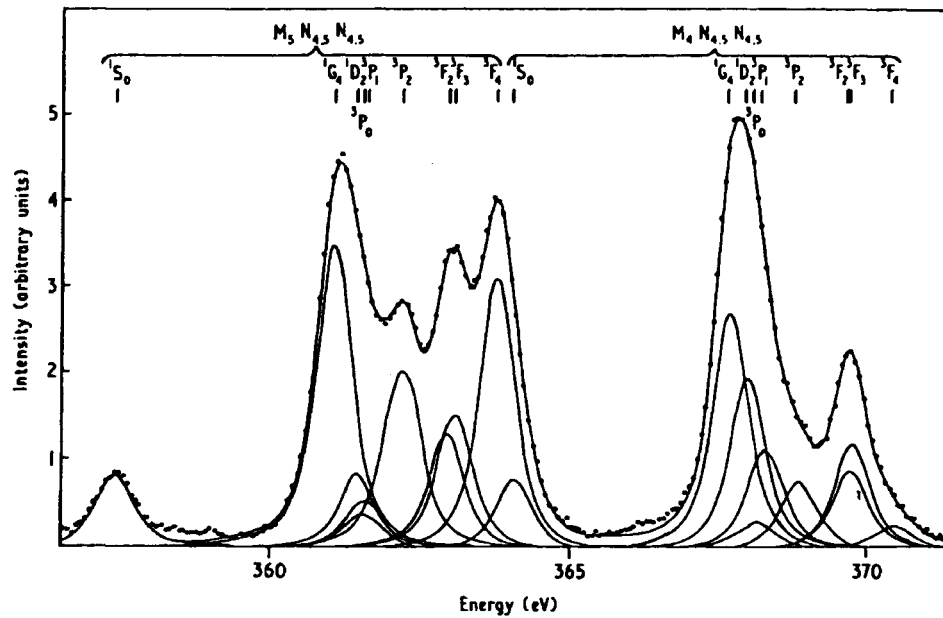


Figure 3.13 Fine structure in the $M_{4,5}N_{4,5}N_{4,5}$ Auger spectrum of cadmium due to multiplet splittings in the final state of the Auger process. The upper part is the observed spectrum with the assumed inelastic background shown as the dashed line. The lower part shows the calculated positions and intensities of the various multiplet components for each group, with the resultant theoretical envelope (solid line) compared with the experimental points. (Reproduced from Aksela and Aksela¹⁴ by permission of the Institute of Physics)

Data more difficult to interpret than XPS

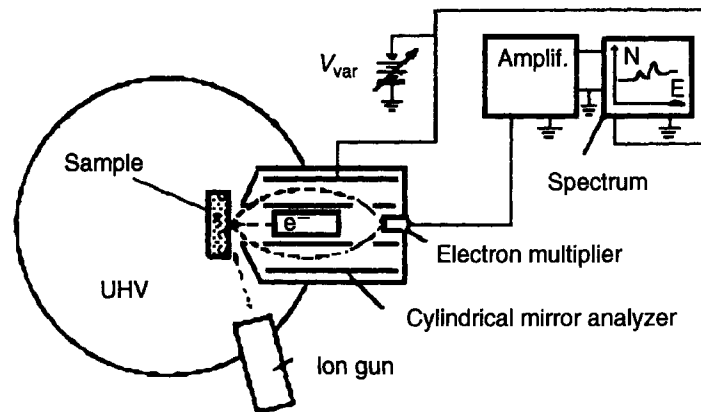
Some current theory investigations looking at Auger lineshapes

Potentially rich spectra - may be able to get many energy levels from single Auger peak envelope

AES not used as much as XPS for chemical environment information

Used extensively for quantitative compositional analysis

5.9 Instrumentation for AES



Electron (or x-ray) source, sample, electron energy analyzer (monochromator), electron detector, readout and data processing

5.9.1 Electron Sources (Electron Guns)

Two common types (i) thermionic emission (ii) field emission

- (i) thermionic emission is based on Boltzmann distribution of electron energies in metal

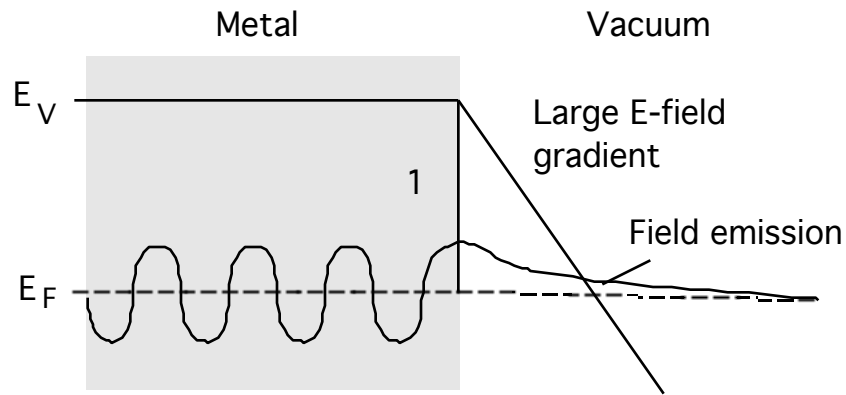
at high temperature, small fraction of electron have enough energy to escape

typical heated filament materials include W, W(Ir) or LaB₆ - low

- (ii) field emission guns (FEG)

use large electric field gradients to remove electrons by tunneling

emission material fashioned to sharp point for best electron flux and beam diameter



In both type:

Lenses electrostatically manipulate beam - extract, collimate, focus and scan (deflection plates)

Minimum diameters of 20 nm can be achieved with care

Current >10 mA to <1 nA used (*space-charge effects* limit current at low beam energies and diameter)

5.9.2 Electron Energy Analyzers

Since Auger peaks are generally broader than photoemission peaks

- do not need high resolution analyzer (concentric hemispherical analyzer - CHA)
- do need good (angular) collection efficiency

Cylindrical Mirror Analyzer (CMA):

- Single or double-pass (higher resolution)
- Large angular acceptance
- Often contain integral electron gun
- Scanned by varying potentials on inner and outer cylinders
- No retarding to fixed pass energy so analyzer resolution varies with electron KE (but still less than peak FWHM)

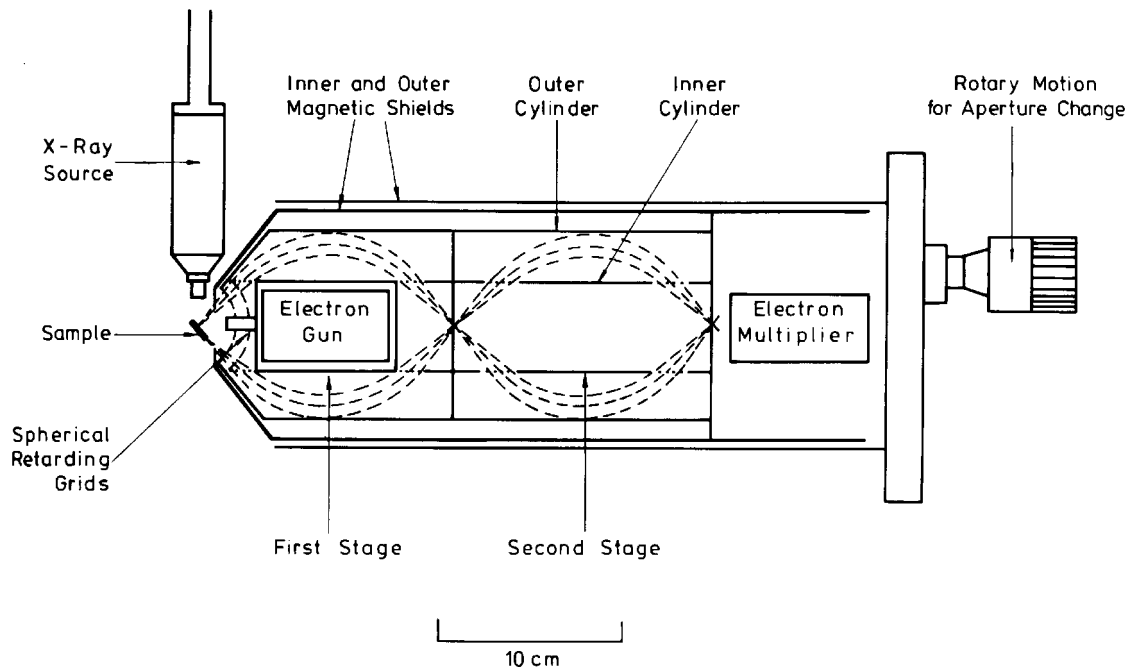


Figure 2.29 Diagram of a double-pass CMA, used for both XPS and AES. Electrons are retarded to a constant pass energy for XPS via two spherical grids at the entrance to the first stage, centred on the source area on the sample. The exit aperture of the first stage constitutes the entrance aperture to the second stage. The entrance and exit apertures to the second stage can be changed remotely through an external rotary motion drive. For AES the retard grids are grounded, and so is the inner cylinder. (Reproduced from Palmberg²² by permission of Elsevier Scientific Publishing Company)

5.10 Applications of AES

5.10.1 Quantitative AES

$$I_a = \text{electrons}(x, y) \times P_{\text{backscatter}}(E, \text{material}) \\ \times C_a(x, y, d) \times \sigma_a(E, n, l) \times P_{\text{Auger}}(ABC) \\ \times P_{\text{no-loss}}(\text{material}, d) \times A_{\text{analyzer}} \times T_{\text{analyzer}}(KE)$$

where

$\text{electrons}(x, y)$ - incident electron flux

$P_{\text{backscatter}}(E, \text{material})$ - proportion electrons backscattered causing additional Auger electrons

$C_a(x, y, d)$ - concentration of element a

$\sigma_a(E, n, l)$ - subshell (*core hole*) ionization cross-section

$P_{\text{Auger}}(ABC)$ - probability of Auger process defined by three sets of quantum numbers

$P_{\text{no-loss}}(\text{material}, d)$ - probability of no-loss escape

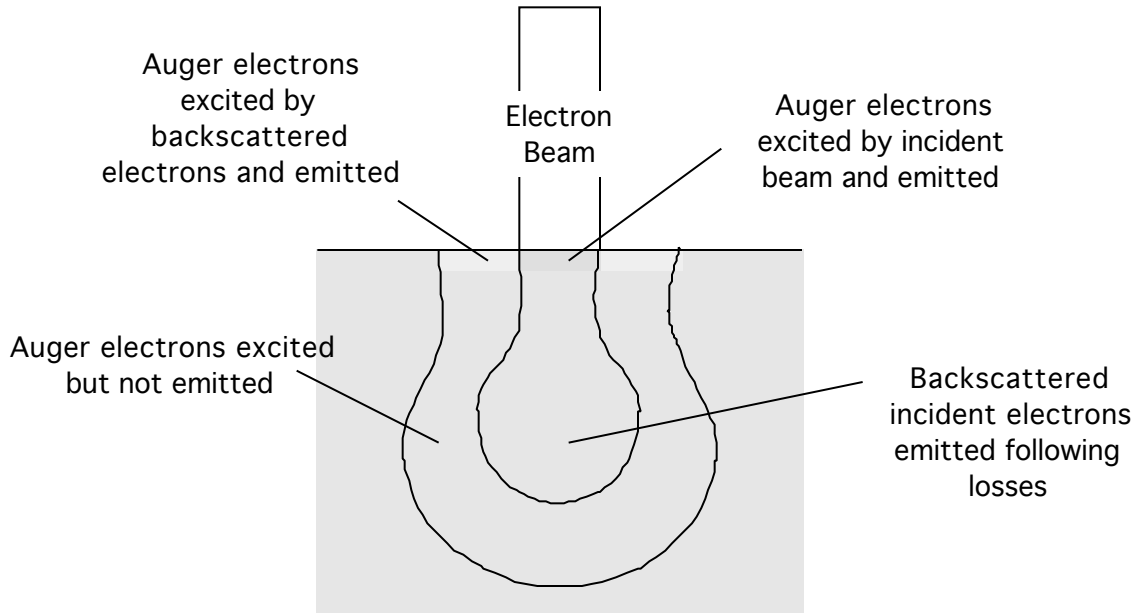
A_{analyzer} - angular acceptance of analyzer

$T_{\text{analyzer}}(KE)$ transmission function of analyzer

Many factors similar to XPS

- extra terms $P_{\text{backscatter}}$ and $P_{\text{Auger}}(ABC)$
- incident electron energy (E) is variable (1-5 keV)
- $P_{\text{backscatter}}$ is complex function of material and incident energy - difficult to calculate

- electrons detected from outside irradiated area due to backscattered electrons
- diameter of analyzed area $2-5 \times$ irradiated area



Empirical observations of ρ_a versus E and Z produce useable estimates for composition (though may be up to 50 % inaccurate)

Table 4.3. AES transitions and their relative sensitivity factors

Atomic Number	Element	Atomic Volume A/ρ^* [$\times 10^{-6} \text{ m}^3 / \text{mol}$]	AES transition	Kinetic Energy of AES transition (eV)
1	H	14.1		
2	He	31.8		
3	Li	13.1		
4	Be	5.0		
5	B	4.6		
6	C	5.3		
7	N	17.3		
8	O	14		
9	F	17.1		
10	Ne	16.8		
11	Na	23.7		
12	Mg	14.0		
13	Al	10.0		
14	Si	12.1		
15	P	17.0		
16	S	15.5		
17	Cl	18.7		
18	Ar	24.2		
19	K	45.3		
20	Ca	29.9		
21	Sc	15.0		
22	Ti	10.6		
23	V	8.35		
24	Cr	7.23		
25	Mn	7.39		
26	Fe	7.1		
27	Co	6.7		
28	Ni	6.6		
29	Cu	7.1		
30	Zn	9.2		
31	Ga	11.8		
32	Ge	13.6		
33	As	13.1		
34	Se	16.5		
35	Br	23.5		
36	Kr	32.2		
37	Rb	55.9		
38	Sr	33.7		
39	Y	19.8		
40	Zr	14.1		
41	Nb	10.8		
42	Mo	9.4		
43	Tc			
44	Ru	8.3		
45	Rh	8.3		
46	Pd	8.9		
47	Ag	10.3		
48	Cd	13.1		
49	In	15.7		
50	Sn	16.3		
51	Sb	18.4		
52	Te	20.5		
53	I	25.7		
54	Xe	42.9		
55	Cs	70		
56	Ba	39		
57	La	22.5		
58	Ce	21.0		
59	Pr	20.8		
60	Nd	20.6		
61	Pm			
62	Sm	19.9		
63	Eu	28.9		
64	Gd	19.9		
65	Tb	19.2		
66	Dy	19.0		
67	Ho	18.7		
68	Er	18.4		
69	Tm	18.1		
70	Yb	24.8		
71	Lu	17.8		
72	Hf	13.6		
73	Ta	10.9		
74	W	9.53		
75	Re	8.85		
76	Os	8.43		
77	Ir	8.54		
78	Pt	9.10		
79	Au	10.2		
80	Hg	14.8		
81	Tl	17.2		
82	Pb	18.3		
83	Bi	21.3		
84	Po	22.7		
85	At			
86	Rn			
87	Fr			
88	Ra	45		
89	Ac			
90	Th	19.9		
91	Pa	15.0		
92	U	12.5		
93	Np			
94	Pu			
95	Am			
96	Cm			
97	Bk			
98	Cf			
99	Es			
100	Fm			
101	Mn	1175		
102	Fe	1126		
103	Co	1073		
104	Ni	1024		
105	Cu	976		
106	Zn	928		
107	Ga	880		
108	Ge	832		
109	As	784		
110	Se	736		
111	Br	688		
112	Kr	640		
113	Rb	592		
114	Sr	544		
115	Y	496		
116	Zr	448		
117	Nb	400		
118	Mo	352		
119	Tc	304		
120	Ru	256		
121	Rh	208		
122	Pd	160		
123	Ag	112		
124	Cd	64		
125	In	16		
126	Sn	8		
127	Sb	4		
128	Te	2		
129	I	1		
130	Xe	0.5		
131	Ba	0.25		
132	La	0.125		
133	Ce	0.0625		
134	Pr	0.03125		
135	Nd	0.015625		
136	Pm	0.0078125		
137	Sm	0.00390625		
138	Eu	0.001953125		
139	Gd	0.0009765625		
140	Tb	0.00048828125		
141	Dy	0.000244140625		
142	Ho	0.0001220703125		
143	Er	0.00006103515625		
144	Tm	0.000030517578125		
145	Yb	0.0000152587890625		
146	Lu	0.00000762939453125		
147	Hf	0.000003814697265625		
148	Ta	0.0000019073486328125		
149	W	0.00000095367431640625		
150	Re	0.000000476837158203125		
151	Os	0.0000002384185791015625		
152	Ir	0.00000011920928955078125		
153	Pt	0.000000059604644775390625		
154	Au	0.0000000298023223876953125		
155	Hg	0.00000001490116119384765625		
156	Tl	0.000000007450580596923828125		
157	Pb	0.0000000037252902984619140625		
158	Bi	0.00000000186264514923095703125		
159	Po	0.000000000931322574615478515625		
160	At	0.00000000046566128730773928125		
161	Rn	0.000000000232830643653869640625		

- relative sensitivity factors (RSF)

$$I_{\text{true}} = \frac{I_{\text{measured}}}{\text{RSF}}$$

- approximately compensate for $P_{\text{backscatter}}$, P_{Auger} , P_a and $P_{\text{no-loss}}$ at fixed E

But must be measured under identical conditions to reduce uncertainty in $P_{\text{backscatter}}$

Best method for quantitative AES is to standardize using known system

In the case of monolayer films it is possible to remove uncertainties in $P_{\text{backscatter}}$ by comparison with other techniques

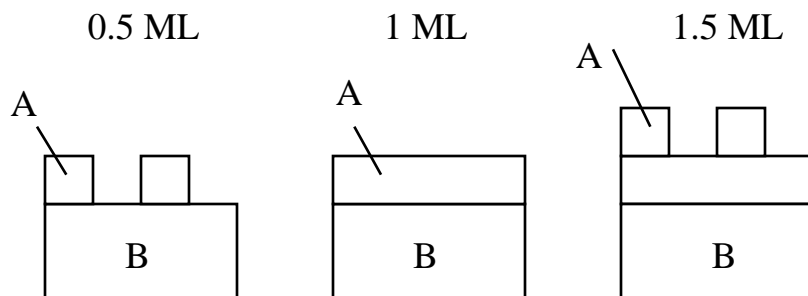
- electrochemical (cyclic voltametry)
- desorption measurements
- electron diffraction (LEED or RHEED)

5.10.2 Film Growth Mechanisms

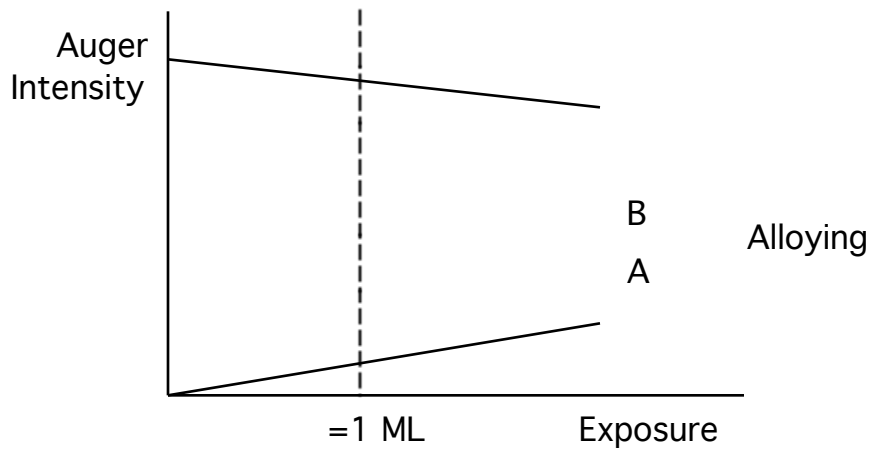
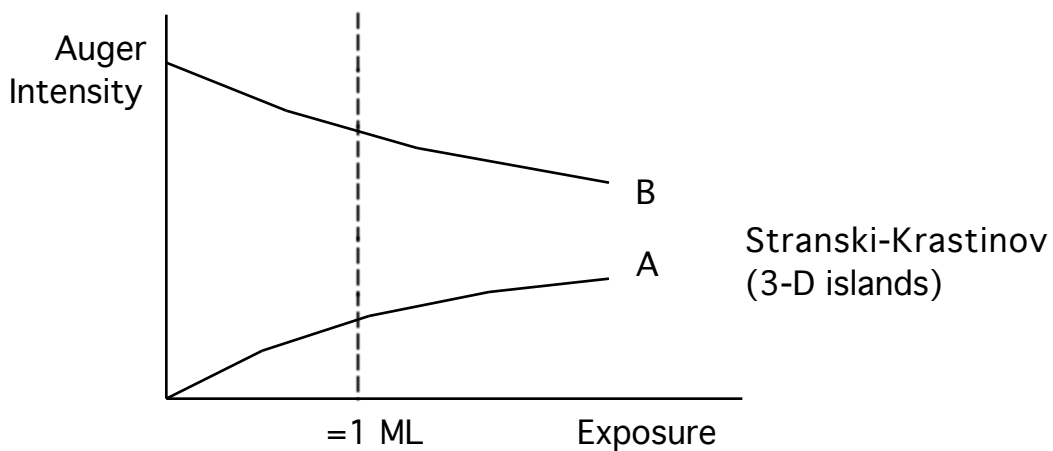
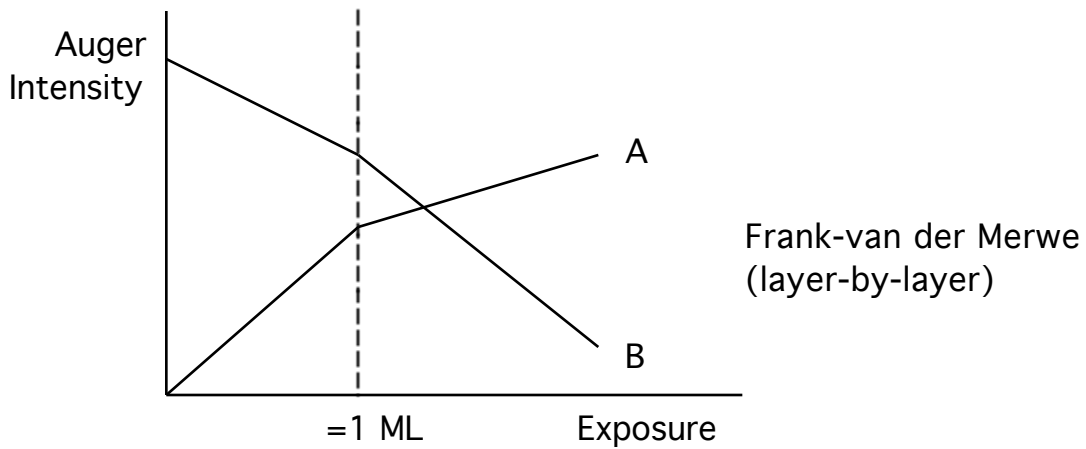
AES signals in layer-by-layer growth?

Linear decrease in B due to attenuation

Linear increase in A submonolayer as concentration increases



Slower increase in A after 1 ML due to attenuation of second layer



In principle, can determine growth mode by examining behavior of AES (or XPS) signal with exposure - ignores changes in sticking probability S

$$S = \frac{\# \text{ species that remain adsorbed}}{\# \text{ species that strike surface}} \quad 0 < S < 1$$

5.10.3 Elemental Mapping - The Scanning Auger Microprobe (SAM)

Electron beam can be rapidly scanned in *x or y* direction across surface

- line scan
- monitor intensity of Auger peaks as function of *x* or *y* position

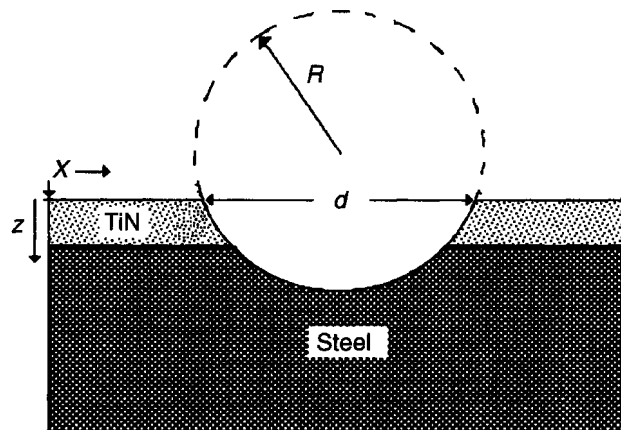


Figure 4.19. Section of a stainless steel sample covered with a layer of TiN of thickness d . The vertical arrows indicate the limits of displacement of the electron beam

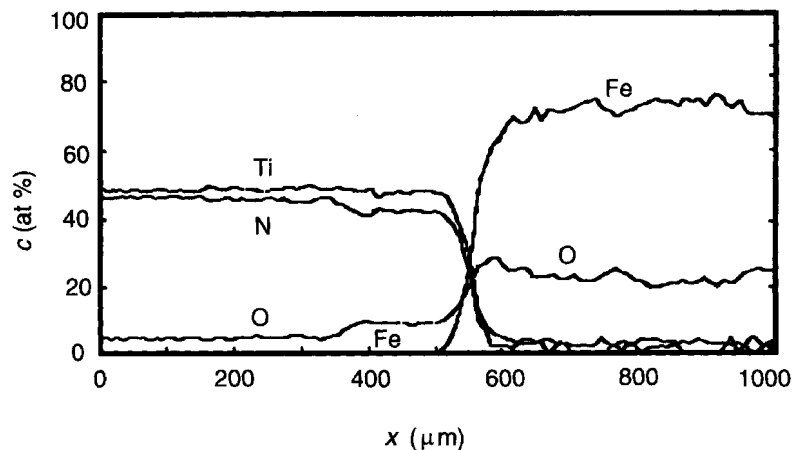


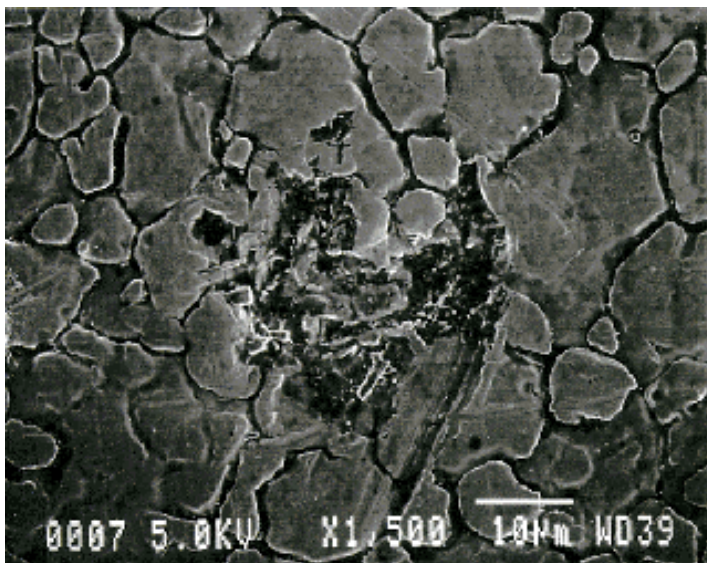
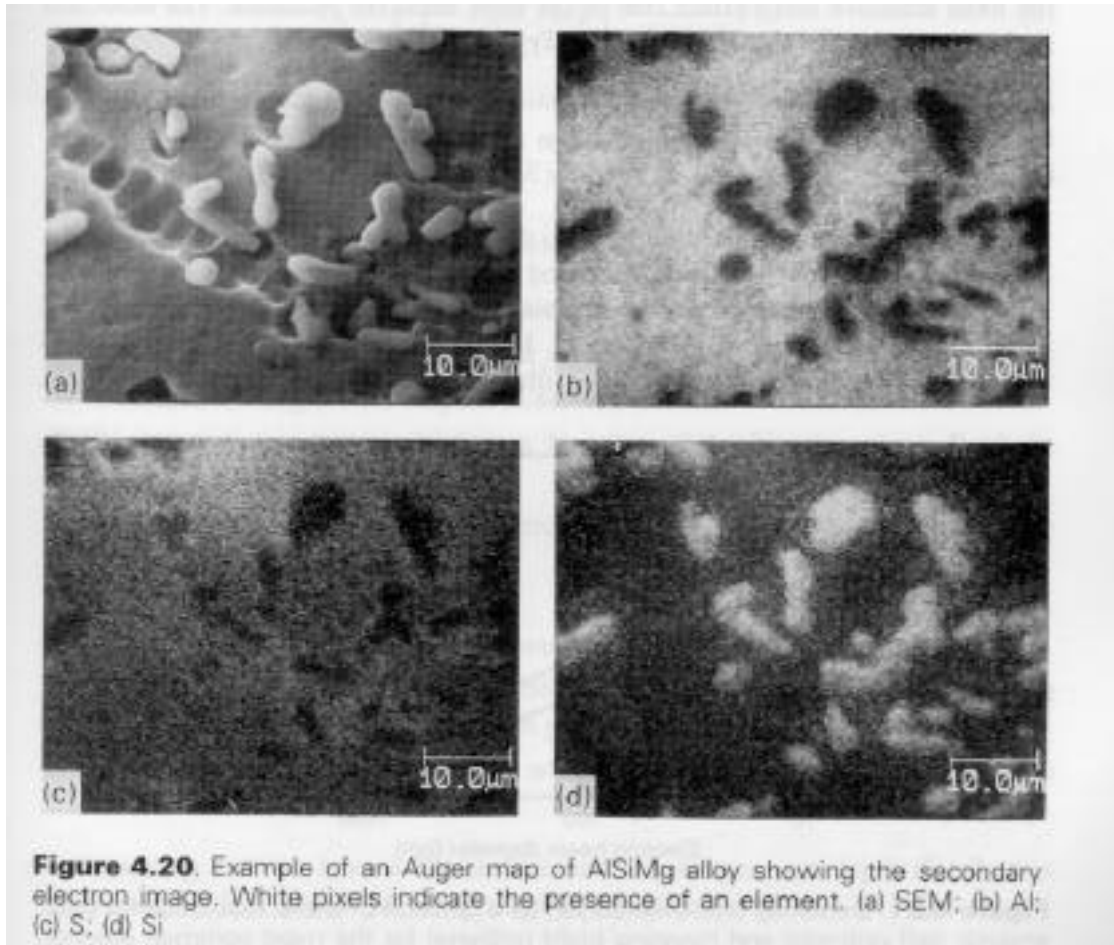
Figure 4.18. Example of a line scan over the crater edge produced by ball cratering showing the atomic concentration as a function of the displacement of the electron beam. The crater edge is located approximately at $x = 500 \mu\text{m}$

- need narrow primary electron beam (affects lateral resolution)

If primary beam is scanned in *x and y* directions

- can map elemental composition

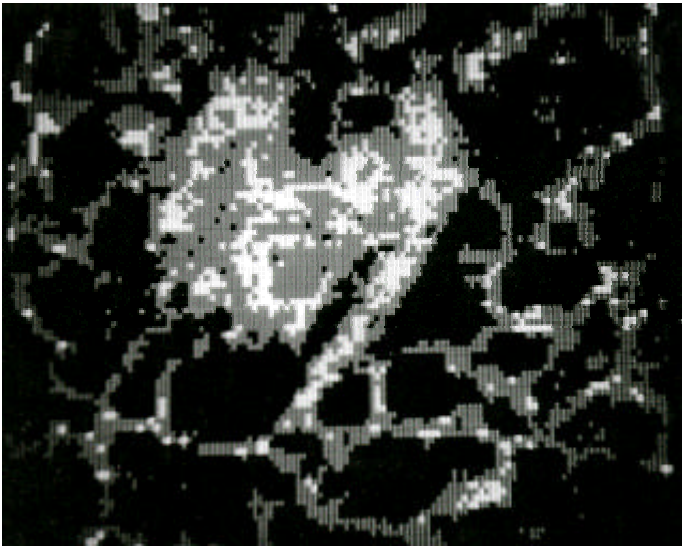
- scanning Auger microprobe
- resolution $<1 \mu\text{m}$ possible
- image acquired in $<10 \text{ s}$ (dynamic surfaces?)



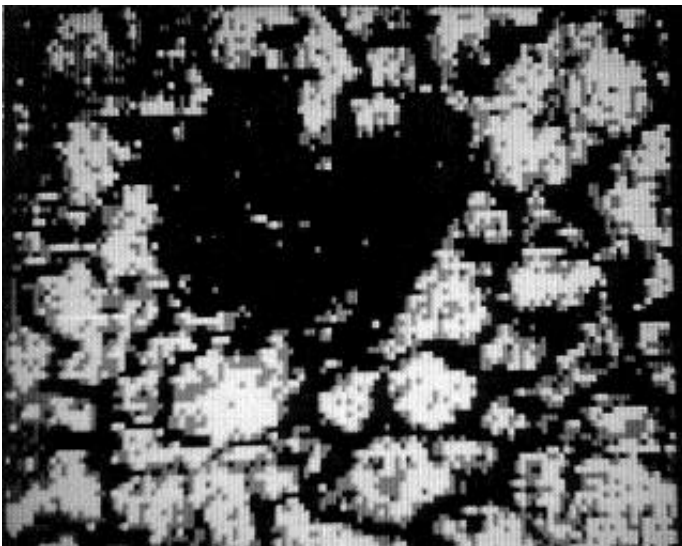
Scanning electron
micrograph (SEM) image
of surface defect (etch pit)
on stainless steel



SAM Fe LMM Auger
image



SAM C KLL Auger
image



SAM O KLL Auger
image

5.11 Summary

Simple and inexpensive instrumentation

- electron gun and CMA
- XPS instrumentation (x-ray source and CHA)
- modified LEED apparatus (RFA)

Rapid analysis with good S/N (especially $N'(E)$ and $N''(E)$ spectra)

- typically faster than XPS

Sensitive to all elements except H and He, sensitivity <1% of ML for low Z elements ($<10^{13}$ atoms·cm⁻²)

- can vary sensitivity somewhat by changing incident beam energy

Precision better than 5 %

Extensively used for elemental mapping (SAM) with < 1 μm resolution (minimum ~50 Å)

- much easier than x-ray beam

Semi-quantitative (especially if used with standards)

Some chemical shift information

BUT

Auger spectrum must be differentiated for good sensitivity

One electron picture less reliable than XPS

- Chemical shift information embedded in complex spectra
- Multiple final states/loss features produce complex/broadened spectra

Large electron flux may induce chemistry in sensitive materials

Lateral resolution of incident beam always degraded in analyzed beam

- focus to $<1 \mu\text{m}$ not trivial

Relative sensitivity factors alone produce estimates of composition only (50%) without careful standardization